PHOTOCATALYTIC ACTIVITY OF RUGBY-LIKE Nd-DOPED ZnO PARTICLES ACTIVATED BY ULTRAVIOLET

A. PHURUANGRAT[a,*], T. THONGTEM[b,c], S. SATCHAWAN[e],
S. THONGTEM[b,d]

[a]*Department of Materials Science and Technology, Faculty of Science,
Prince of Songkla University, Hat Yai, Songkhla 90112, Thailand*
[b]*Materials Science Research Center, Faculty of Science, Chiang Mai University,
Chiang Mai 50200, Thailand*
[c]*Department of Chemistry, Faculty of Science, Chiang Mai University,
Chiang Mai 50200, Thailand*
[d]*Department of Physics and Materials Science, Faculty of Science,
Chiang Mai University, Chiang Mai 50200, Thailand*
[e]*Department of Chemistry, Faculty of Science,
Chandrakasem Rajabhat University, Chatuchak, Bangkok 10900*

0–3 wt% Nd-doped ZnO particles were synthesized by microwaving through aqueous solutions containing Zn^{2+} ions and different contents of Nd^{3+} ions in deionized water. The products were characterized by X-ray diffraction (XRD), scanning electron microscopy (SEM), Raman spectroscopy and Fourier-transform infrared spectroscopy (FTIR), and were specified as hexagonal wurtzite ZnO particles. Their photocatalytic activities were investigated through the degradation of methylene blue (MB) activated by UV radiation. In this research, 3 wt% Nd-doped ZnO showed the best significantly improved photocatalytic activity for degradation of MB dye of 3.95 x 10^{-3} min^{-1}. The photocatalysis of Nd-doped ZnO samples activated by UV radiation was also discussed.

1. Introduction

In recent years, wastewater from printing and dyeing factories has become an important environmental problem because natural resources contain a number of toxic organic compounds with low biodegradability (~10–15 %) which can cause cancer and mutation to humans via the food chain [1, 2]. Semiconducting photocatalysts have been applied to purify those of printing and dyeing contaminants containing in wastewater activated by solar light irradiation. Zinc oxide (ZnO) with a direct band gap at 300 K of 3.37 eV and a large exciton binding energy of 60 meV has been widely studied for photocatalysis due to its high photosensitivity, inexpensive, excellent chemical and mechanical stability, and abundant availability [2–5]. Nevertheless, photocatalytic performance of ZnO is limited by rapid recombination of photo-generated electron-hole pairs [5, 6]. Thus, metal-doped ZnO is an excellent method for improving the photocatalytic efficiency of ZnO by hindering recombination of electron–hole pairs [7, 8]. In this research, Nd-doped ZnO photocatalysts were synthesized by microwaving through the different precursor solutions and were applied for photodegradation of methylene blue (MB) under UV radiation.

---

*Corresponding authors: phuruangrat@gmail.com

2. Experimental procedure

0–3 wt% Nd-doped ZnO samples were synthesized by microwave-assisted solution method using zinc nitrate hexahydrate ($Zn(NO_3)_2 \cdot 6H_2O$), neodymium nitrate hexahydrate ($Nd(NO_3)_3 \cdot 6H_2O$) and sodium hydroxide (NaOH). 0.01 mole $Zn(NO_3)_2 \cdot 6H_2O$ and 0–3 wt% $Nd(NO_3)_3 \cdot 6H_2O$ were separately dissolved in 100 ml deionized water. The solutions containing the dissolved salts were further mixed with constant stirring and the mixed solutions were adjusted the pH to 9 by 3 M NaOH. These solutions were put in a microwave oven and were heated by 300 W microwave for 20 min. The precipitates were collected, washed and dried at 80 ^{o}C for 24 h.

X-ray diffraction (XRD) patterns of the products were analyzed by a PANalytical X'pert Pro MPD diffractometer with a monochromatic Cu K_{α} radiation (λ = 1.54056 Å). Scanning electron microscopic (SEM) images were taken by a JEOL, JSM 6335F SEM coupled with an Oxford INCA energy dispersive spectrometer (EDS) operating at 20 kV. Fourier transform infrared (FTIR) spectra of the samples were recorded by a Bruker Tensor 27 FTIR spectrometer. Raman spectra was characterized by a HORIBA Jobin Yvon T64000 spectrophotometer using 30 mW HeNe laser with 632.8 nm red wavelength.

Photocatalytic activities of the as-prepared ZnO and Nd-doped ZnO samples were investigated through photodegradation of methylene blue (MB) aqueous solutions at room temperature under three 18 W black light fluorescent tubes (PICCOZZO) as a UV source. 0.02 g photocatalyst was dispersed in 200 ml of 1×10^{-5} M MB aqueous solution in a beaker and stirred in the dark for 30 min to ensure the establishment of adsorption−desorption equilibrium of the dye on the catalytic surface. During UV light irradiation, 5 ml of MB solution was sampled for every 60 min and centrifuged to precipitate the contaminant containing in the solution. The concentration of MB was determined by a UV-visible spectrometer (Perkin Elmer Lambda 25) at a λ_{max} of 664 nm. The photocatalytic degradation efficiency was calculated by the following.

$$\text{Photocatalytic efficiency} = \frac{C_0 - C_t}{C_0} \times 100 \tag{1}$$

where C_0 is the initial absorbance (concentration) of MB solution at equilibrium and C_t is the dye solution absorbance at a certain reaction period.

3. Results and discussion

The XRD patterns of undoped ZnO and Nd-doped ZnO samples are shown in Fig. 1. All peaks of the undoped ZnO sample was assigned to the pure phase of hexagonal structure of wurtzite ZnO (JCPDS Card No. 36-1451 [9]). No other peaks were detected by the XRD, indicating the superior purity of the ZnO simple. Obviously, the obtained Nd-doped ZnO samples exhibit the same XRD patterns as that of the pure wurtzite ZnO structure. The results implied that the introduction of Nd dopant did not change the crystalline structure of ZnO. The main diffraction peaks of Nd-doped ZnO samples were shifted to lower angle due to the difference of ionic radii between Nd^{3+} (0.983 Å) and Zn^{2+} (0.74 Å) [8]. In conclusion, Nd^{3+} ions substituted for Zn^{2+} ions containing in ZnO lattice, resulting to an expansion of the ZnO unit cells. The crystallite size (D) was calculated from the (101) orientation using the Scherrer formula.

$$D = \frac{0.9\lambda}{\beta \cos\theta} \tag{2}$$

where λ is the X-ray wavelength, θ is the Bragg diffraction angle corresponding to the (101) peak and β is the peak width at the half maximum (full width at half maximum) [7, 10]. Calculated crystallize sizes of the pure ZnO and 3 wt% Nd-doped ZnO samples were 45 and 49 nm, respectively.
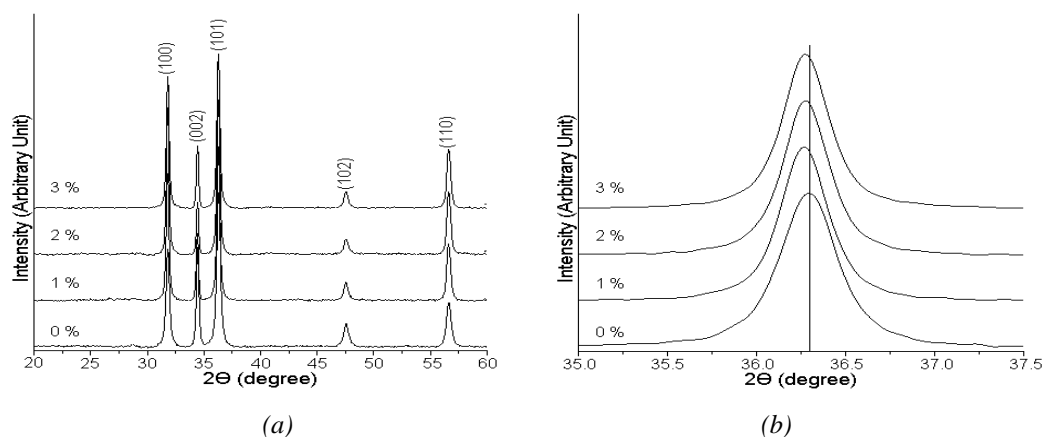
Fig. 1. XRD patterns of ZnO, 1 wt% Nd-doped ZnO, 2 wt% Nd-doped ZnO and 3 wt% Nd-doped ZnO at 2θ of (a) 20°–60° and (b) 35.0^o–37.5^o.

Hexagonal wurtzite ZnO belongs to the C^4_{6v} space group. The group theory predicted that optical phonon at the central point of Brillouin zone belongs to the irreducible representation: $\Gamma = 1A_1 + 2B_1 + 1E_1 + 2E_2$. Both A_1 and E_1 vibration modes are polar and split into transverse (T) and longitudinal (L) optical (O) phonons with different frequencies. Two non-polar E_2 modes are only Raman active. Two B_1 modes are infrared (IR) and Raman inactive (silent mode) [7, 11–14]. Fig. 2a shows Raman spectra of ZnO and Nd-doped ZnO. The sharp Raman peak of pure ZnO at 436 cm^{-1} corresponds to the E_{2H} mode of hexagonal wurtzite ZnO. Clearly, the E_{2H} mode of Nd-doped ZnO was shifted to 422 cm^{-1} due to lattice distortion caused by the substitution of Nd dopant for Zn containing in ZnO crystal. The weak peak at 326 cm^{-1} and the smaller shoulder at 574 cm^{-1} can be assigned to the $E_{2H} - E_{2L}$ and E_1 (LO) modes associated with defects in crystalline ZnO such as ionic deficiency and interstitials [7, 11–14]. The FTIR spectra of ZnO and Nd-doped ZnO are shown in Fig. 2b. They show a broad band at approximately 3442–3212 cm^{-1} specified as the stretching vibration of O–H groups [2, 8]. The rather sharp band at 422 cm^{-1} is assigned to Zn–O bonding of ZnO lattice [2, 8, 13].
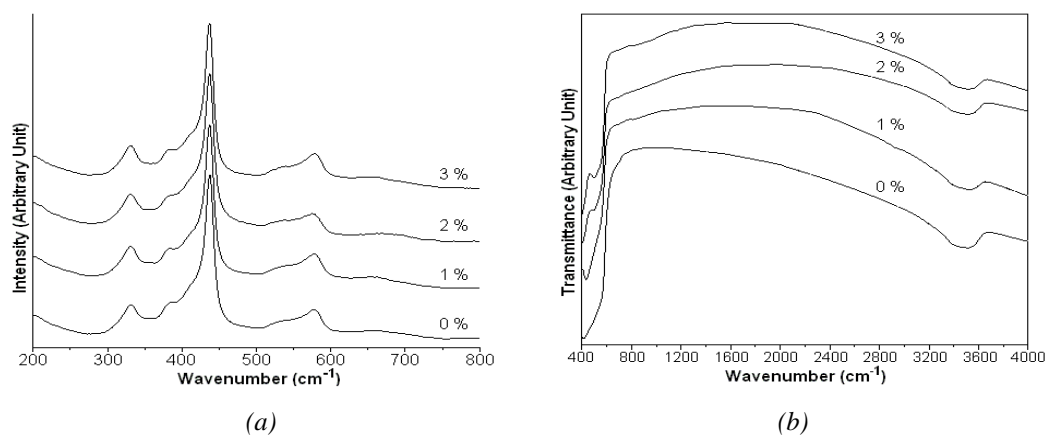
Fig. 2. (a) Raman and (b) FTIR spectra of ZnO, 1 wt% Nd-doped ZnO, 2 wt% Nd-doped ZnO and 3 wt% Nd-doped ZnO.

Different morphologies of ZnO with and without Nd dopant were characterized by SEM as the results shown in Fig. 3. The pure ZnO sample was composed of microflowers of nanoparticles mixed with some nanoparticles with less than 50 nm diameter. For the 3 wt% Nd-doped ZnO sample, the microflowers of ZnO nanoparticles were transformed into microrugbies of nanoparticles. This phenomenon is influenced by Nd-assistant segregation of microflowers. The 3

wt% Nd-doped ZnO sample was composed of nanoparticles clustered together in the shape of microrugbies and irregular-shaped colonies. The chemical composition of the Nd-doped ZnO sample was certified by EDS. The Nd concentration in 3 wt% Nd-doped ZnO sample was detected to be 2.78 % by weight. Obviously, the quantitative EDS analysis revealed that the content of Nd dopant was slightly less than that obtained from the experimental procedure.
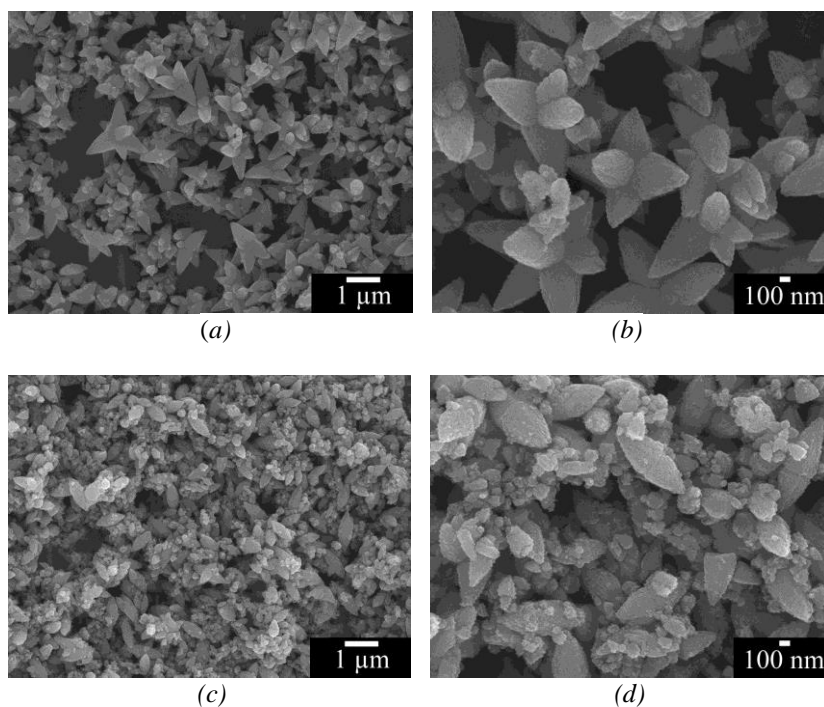
Fig. 3. SEM images of (a, b) ZnO and (c, d) 3 wt% Nd-doped ZnO.

Decolorization efficiency of pure ZnO and Nd-doped ZnO photocatalysts were investigated by evaluating the degradation of methylene blue (MB) as a model contaminant activated by ultraviolet irradiation, as the results shown in Fig. 4a. The color of MB dye was continuously decolorized by both the pure and Nd-doped ZnO photocatalysts activated by UV radiation. The Nd-doped ZnO has higher decolorization rate than the pure one. The decolorization performance of 3 wt% Nd-doped ZnO sample was 71 % within 300 min of UV light irradiation. Photodegradation of MB by the photocatalysts followed the first-order rate law [1, 8]. Fig. 4b shows the plot of $\ln(C_0/C_t)$ versus time for photocatalytic performance of pure ZnO and Nd-doped ZnO in degradation of methylene blue under UV radiation. The plots were fitted to linear lines, suggesting the photodegradation reaction that follows the first-order rate law for photocatalysis. The calculated rate constant values of ZnO, 1 wt% Nd-doped ZnO, 2 wt% Nd-doped ZnO and 3 wt% Nd-doped ZnO were 1.79×10^{-3}, 2.42×10^{-3}, 3.14×10^{-3} and 3.95×10^{-3} min^{-1}, respectively. The last one shows the highest rate constant. The inhibition of photogenerated electron–hole recombination in Nd-doped ZnO scavengers can be explained by the following.

$$\text{Nd}^{3+} + \text{O}_2 + \text{h}\nu \rightarrow \text{Nd}^{4+} + {}^{\bullet}\text{O}_2^{-} \tag{3}$$

$$\text{Nd}^{4+} + \text{e}^{-} \rightarrow \text{Nd}^{3+} \tag{4}$$

$${}^{\bullet}\text{O}_2^{-} + \text{H}^{+} \rightarrow {}^{\bullet}\text{O}_2\text{H} \tag{5}$$

$$2{}^{\bullet}\text{O}_2\text{H} \rightarrow \text{H}_2\text{O}_2 + \text{O}_2 \tag{6}$$
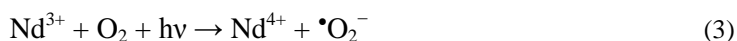
Under UV light irradiation, Nd^{3+} ions reacted with the adsorbed O_2 molecules on surface of Nd-doped ZnO to form Nd^{4+} and ${}^\bullet O_2^-$. The as-produced Nd^{4+} species captured photogenerated electrons in conduction band of ZnO to form Nd^{3+}. Later on, the as-produced ${}^\bullet O_2^-$ and ${}^\bullet O_2 H$ radicals as strong oxidants transformed MB dye into CO_2 and H_2O as final products [15, 16].

(a)   *(b)*
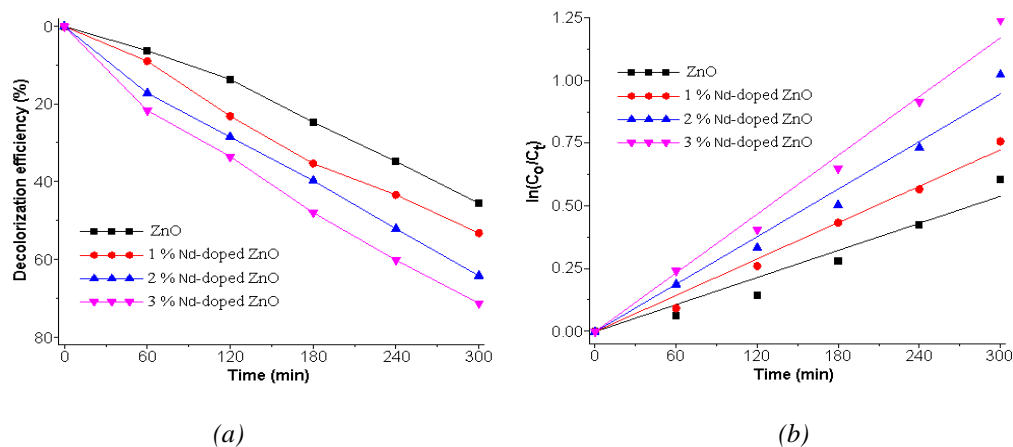
Fig. 4 (a) Decolorization efficiency and (b) $ln(C_0/C_t)$ of ZnO, 1 wt% Nd-doped ZnO, 2 wt% Nd-doped ZnO and 3 wt% Nd-doped ZnO for different lengths of UV irradiation time.

4. Conclusions

In summary, ZnO and Nd-doped ZnO were successfully synthesized by microwave-assisted method. Phase, morphology and vibration mode of the as-prepared ZnO and Nd-doped ZnO products were certified by XRD, FE-SEM, Raman and FTIR analyses. The Nd-doped ZnO samples displayed significantly improved photodegradation in removing of MB dye activated by UV radiation, attributed to inhibit the recombination of photogenerated electron–hole pairs.

Acknowledgments

References

[1] Q. Chen, Y. Zhang, D. Zhang, Y. Yang, J. Water Process Eng. **16**, 14 (2017).
[2] H. K. Seo, H.S. Shin, Mater. Lett. **159**, 265 (2015).
[3] P. Samadipakchin, H. R. Mortaheb, A. Zolfaghari, J. Photochem. Photobiol. A **337**, 91 (2017).
[4] M. Cao, F. Wang, J. Zhu, X. Zhang, Y. Qin, L. Wang, Mater. Lett. **192**, 1 (2017).
[5] B. Pant, M. Park, H.Y. Kim, S.J. Park, Synth. Metals **220**, 533 (2016).
[6] L. Wang, X. Hou, F. Li, G. He, L. Li, Mater. Lett. **161**, 368 (2015).
[7] W. Bousslama, H. Elhouichet, M. Férid, Optik **134**, 88 (2017).
[8] O. Yayapao, T. Thongtem, A. Phuruangrat, S. Thongtem, Mater. Lett. **90**, 83 (2013).
[9] Powder Diffract. File, JCPDS-ICDD, 12 Campus Bld., Newtown Square, PA 19073-3273, U.S.A., (2001).
[10] R. O. Yathisha, Y. Arthoba Nayaka, C. C. Vidyasagar, Mater. Chem. Phys. **181**, 167 (2016).
[11] C. Mrabet, O. Kamoun, A. Boukhachem, M. Amlouk, T. Manoubi, J. Alloy. Compd. **648**, 826 (2015).
[12] A. Phuruangrat, S. Thongtem, T. Thongtem, Mater. Des. **107**, 250 (2016).

630

[13] A. J. Reddy, M. K. Kokila, H. Nagabhushana, J. L. Rao, C. Shivakumara, B. M. Nagabhushana, R. P. S. Chakradhar, Spectrochim. Acta A **81**, 53 (2011).

[14] M. Kahouli, A. Barhoumi, A. Bouzid, A. Al-Hajry, S. Guermazi, Superlatt. Microst. **85**, 7 (2015).

[15] A. R. Khataee, A. Karimi, R. D. C. Soltani, M. Safarpour, Y. Hanifehpour, S. W. Joo, Appl. Catal. A. **488**, 160 (2014).

[16] O. Bechambi, L. Jlaiel, W. Najjar, S. Sayadi, Mater. Chem. Phys. **173**, 95 (2016).